New Auxiliary Variable-Based ADMM for Nonconvex AC OPF

Miao Zhang, Rabi Shankar Kar, Zhixin Miao Lingling Fan

Department of Electrical Engineering, University of South Florida, Tampa FL USA 33620.

Email: linglingfan@usf.edu.

Abstract

The main challenge in implementing alternating direction method of multipliers (ADMM) for nonconvex alternating current optimal power flow (AC OPF) is that ADMM method does not guarantee convergence for nonconvex problems. Using auxiliary variables for information exchange among subareas play a critical role in convergence improvement. This paper proposes a new auxiliary variable-based ADMM for nonconvex AC OPF. The proposed approach can improve convergence with less iterations compared with the existing method. The proposed ADMM algorithm is tested for power grids with sizes ranges from 30 buses to 1354 buses. Subareas are generated using spectral clustering based on a graph Laplacian representing network connectivity. The numerical results are compared with those based on the existing auxiliary variables-based method in the literature. Case studies demonstrate improvement in convergence due to the new auxiliary variables.

Keywords: ADMM, AC OPF, spectral partitioning.

1. Introduction

The alternating current optimal power flow (AC OPF) problem is a nonconvex optimization problem. The decision variables include generators' real and reactive power outputs and voltage magnitude and angle at each bus. The objective function is usually the generation cost and the constraints include equality constraints that describe power injection relationship with voltage phasors and inequality constraints that describe generator limits, voltage limits, and line flow limits.

A grid usually has multiple control agents. For the sake of security and privacy, limited information exchange is desired among agents. Thus, distributed OPF is desired [1]. Distributed optimization techniques, e.g., dual decomposition [2], auxiliary problem principal [3, 4], primal-dual decomposition [5], ADMM [6, 7], have been proposed for AC OPF solving. Among them, ADMM gains more and more popularity due to its guaranteed convergence for convex problems [8]. For nonconvex optimization problems, ADMM does not offer guaranteed convergence.

To have a guaranteed convergence, AC OPF problem may be first relaxed to a convex optimization problem. Second-order cone program (SOCP) relaxation is one such methods. SOCP relaxation has been implemented in distribution network AC OPF [9]. In [10, 11, 12, 13], ADMM is used to solve SOCP relaxation of AC OPF for radial networks. Semi-definite programming (SDP) relaxation is a tighter relaxation compared to SOCP relaxation. SDP relaxation of AC OPF has been studied in the literature, e.g., [14, 15, 16, 17]. In [18, 6, 19, 20], ADMM is implemented to solve SDP relaxation of AC OPF.

Instead of using relaxation, research efforts [7, 21, 22, 23] are devoted to implement ADMM directly to the nonconvex AC OPF problems. The main challenge is related to convergence since ADMM does not guarantee convergence for nonconvex problems. In addition, for large-scale power grids, manual partitioning of a grid into multiple subareas is a challenge. Hence, automatic partition has been investigated for distributed AC OPF. Power grids can be partitioned based on generator location [22], tie-lines [24], electrical distance [25], or spectral clustering [26].

In [7], ADMM is implemented for nonconvex AC OPF solving. Shared rectangular voltage coordinates are exchanged among subproblems. In [21], we have solved the IEEE 14-bus system AC OPF problem using

ADMM algorithm. Reference [22] improves ADMM convergence speed by varying penalty parameter and introducing auxiliary variables for regional information exchange. Network partitioning in [22] depends on generators location. In [23], the authors adopt the auxiliary variables proposed in [22] and an intelligent partitioning method based on spectral clusering [27]. The auxiliary variables ($\boldsymbol{z}$) in [22, 23] are constructed to exchange tie-line voltage phasor differences and sums between connecting regions. This approach greatly improves the convergence speed for ADMM of nonconvex AC OPF.

This paper deals with a centralized AC OPF problem and solves this classical problem in a distributed fashion. We further improve the convergence of ADMM for nonconvex AC OPF by introducing a set of new auxiliary variables for regional information exchange. Our proposal is based on a detailed examination of tie-line power flow expressions between two areas. The proposed new auxiliary variables are similar as the decision variables in SOCP relaxation of AC OPF where c_{ij} and s_{ij} are used to replace voltage phasors [9]. We compared the ADMM convergence speed using the new auxiliary variables versus that using the auxiliary variables in [23, 22] and see improvement for all cases we tested.

The rest of the paper is organized as follows. In Section II, ADMM for AC OPF problem is presented in a nutshell with the IEEE 14-bus system being used as an example for illustration of the ADMM algorithm and the information exchange structure. Section III first examines the auxiliary variables in the literature and then proposed a set of new auxiliary variables. Section IV presents the automatic spectral partitioning technique. Section V presents case studies and Section VI concludes this paper.

2. ADMM for AC OPF in a Nutshell

2.1. AC OPF

The AC OPF problem is considered in this paper, where the objective is to minimize the generation cost subject to power flow equality constraints, generator limits, line flow limits and voltage limits. It is a nonconvex optimization problem. The mathematic programming problem is presented in (1).

$$\min_{\boldsymbol{x}} \quad \sum_{i\in\mathcal{G}}(f_{Pi}(P_{gi}) + f_{Qi}(Q_{gi})) \tag{1a}$$

$$\text{s.t.} \quad P_i^g + jQ_i^g - P_i^d - jQ_i^d = S_i(V,\theta), \quad i \in \mathcal{N} \tag{1b}$$

$$S_{ij}^{\min} \le |S_{ij}(V,\theta)| \le S_{ij}^{\max}, \quad (i,j) \in \mathcal{L} \tag{1c}$$

$$P_i^g + jQ_i^g = \sum_{k\in\mathcal{G}_i}(P_{gk} + jQ_{gk}), \quad i \in \mathcal{N} \tag{1d}$$

$$P_{gi}^{\min} \le P_{gi} \le P_{gi}^{\max}, \quad i \in \mathcal{G} \tag{1e}$$

$$Q_{gi}^{\min} \le Q_{gi} \le Q_{gi}^{\max}, \quad i \in \mathcal{G} \tag{1f}$$

$$V_i^{\min} \le V_i \le V_i^{\max}, \quad i \in \mathcal{N} \tag{1g}$$

where $\mathcal{G}$ is the set of all generators, $\mathcal{G}_i$ is the subset of the generators that are connected to Bus i, $\mathcal{N}$ is the set of all buses, $\mathcal{L}$ is the set of all branches. The decision variables include voltage magnitude $V \in \mathbb{R}^{|\mathcal{N}|}$, phase angle vector $\theta \in \mathbb{R}^{|\mathcal{N}|}$, generator's active power and reactive power $P_g \in \mathbb{R}^{|\mathcal{G}|}$ and $Q_g \in \mathbb{R}^{|\mathcal{G}|}$ where $|.|$ notates the cardinality of a set. The decision variable $\boldsymbol{x}$ is defined as: $\boldsymbol{x}^T = [P_g^T \quad Q_g^T \quad V^T \quad \theta^T]^T$.

(1a) presents the objective function as the summation of individual polynomial cost functions $f_{Pi}(P_{gi})$ and $f_{Qi}(Q_{gi})$. (1b) are the power flow equality constraints. P_i^g and Q_i^g are the total real and reactive power generation at Bus i. P_i^d and Q_i^d are the active and reactive load demands at Bus i. (1c) are inequality constraints related to line flow limits. The limits of the generators' power and the network's bus voltages are listed in inequality (1e)-(1g).

The AC OPF is a nonconvex optimization problem due to the nonlinear equality constraints related to complex power injections S_i and the inequality constraints related to line flow S_{ij}.

2.2. ADMM Implementation on IEEE 14-Bus Network

Consensus ADMM has been be implemented in our prior paper [21]. In this subsection, a brief summary of the consensus ADMM in [21] is presented. In consensus ADMM, the original problem will be casted into multiple subproblems. Consensus ADMM has an information aggregation step. At every step, given the information from the aggregator as well as the dual variables, each subproblem finds its decision variables ($\boldsymbol{x}_k$, where k represents k^{th} subproblem) and sends out exchanging information (notated as auxiliary variable) to the aggregator. The aggregator then updates the consensus variable z based on all the information collected from all subareas [8].

In this section, we will examine an example system and formulate ADMM implementation for AC OPF. We then extend the formulation to a general system.

2.2.1. Subsystems Separation

In Fig. 1, the IEEE 14-bus system's network topology is given. It has 5 generators and is partitioned into 3 areas. Each area consists of internal buses, interfacing buses, boundary buses and the branches inside this area as well as tie-lines connecting with neighbor areas.

The system will be decoupled by assuming a voltage source at the boundary bus. Fig. 2 shows a simple system is decoupled into two areas. Area 1 and Area 2 have a tie-line between Bus i and Bus j.

Bus j is treated as a voltage source bus in Area 1. Bus i is treated as a voltage source in Area 2. For Area 1, the subproblem decides voltage phasors at Area 1's internal buses, interfacing buses (Bus i) and boundary buses (Bus j). For Area 2, the subproblem problem decides the voltage phosors at Area 2's internal buses, interfacing buses (Bus j) and boundary buses (Bus i). Both subproblems decides the two voltage phasors at Bus i and Bus j. We notate a consensus area for Area 1 and Area 2 which includes buses i and j. At the aggregation step, voltage phasors of the consensus area should be averaged based on the information from both areas.

2.2.2. Information Exchange Structure

For IEEE 14-bus system, three subareas are identified and notated as: A_1, A_2 and A_3. Three consensus areas are notated as: $A_1 \bigcap A_2$, $A_1 \bigcap A_3$ and $A_2 \bigcap A_3$. There is no any consensus area that is related to all three subareas. A_1 includes buses $\{1, 2, 3, 4, 5, 6, 7, 9\}$ where Bus 6 also belongs to A_3 (Line $5-6$ is the tie-line and Buses 7 and 9 also belong to A_2 (Lines $4-7$ and $4-9$ are tie-lines). We notate the buses in each subarea as:

$$\begin{aligned}
\mathcal{N}_{A_1} &= \{1, 2, 3, 4, 5, 6, 7, 9\} \\
\mathcal{N}_{A_2} &= \{4, 7, 8, 9, 10, 11, 14\} \\
\mathcal{N}_{A_3} &= \{5, 6, 9, 10, 11, 12, 13, 14\} \\
\mathcal{N}_{A_1 \bigcap A_2} &= \{4, 7, 9\} \\
\mathcal{N}_{A_1 \bigcap A_3} &= \{5, 6\} \\
\mathcal{N}_{A_2 \bigcap A_3} &= \{10, 11, 14\}
\end{aligned}$$

Instead of defining one aggregator, for this particular case, we define *three* aggregators since there are three consensus areas. In the aggregation step, once two subareas' decision variables have been updated, the corresponding aggregator will update its variables. The information exchange structure among the three subareas and three aggregators are presented in Fig. 3.

An aggregator collects information related to the consensus variables from two areas. It then updates the consensus variables and sends out the updated consensus variables to the two related areas. Each area then conducts a decision making process based on the inputs from those connected aggregators. The related information is again sent to corresponding aggregators.

2.2.3. ADMM Procedure

Area 1's subproblem will decide the voltage phasors for all buses in Area 1 ($\mathcal{N}_{A_1}$) and the generator outputs for all generators in Area 1 (notated as $\mathcal{G}_{A_1} = \{1, 2, 3\}$). Generators 1, 2 and 3 are in Area 1. If

there are generators connected to its boundary buses, e.g., Bus 6, these generators do not belong to Area 1 since the boundary bus is considered as a voltage source bus for the OPF subproblem for Area 1. The decision variables of Area 1 are listed as follows.

$$\boldsymbol{x}_1 = [P_{g1}, P_{g2}, P_{g3}, Q_{g1}, Q_{g2}, Q_{g3}, V_1, \dots V_7, V_9, \theta_1, \dots \theta_7, \theta_9]^T$$

The consensus variable vector between Area 1 and Area 2 is notated as $\boldsymbol{z}_{1,2}$ when referring to Area 1 and notated as $\boldsymbol{z}_{2,1}$ when referring to Area 2. Similarly, the consensus variable vector between Area 1 and Area 3 is notated as $\boldsymbol{z}_{1,3}$ or $\boldsymbol{z}_{3,1}$.

$$\begin{aligned}\boldsymbol{z}_{1,2} = \boldsymbol{z}_{2,1} &= [V_4, V_7, V_9, \theta_4, \theta_7, \theta_9]^T \\ \boldsymbol{z}_{1,3} = \boldsymbol{z}_{3,1} &= [V_5, V_6, \theta_5, \theta_6]^T\end{aligned}$$

$\boldsymbol{z}_{1,2}$ and $\boldsymbol{z}_{1,3}$ will be aggregated into a vector $\boldsymbol{z}_1$ to notate all the consensus variables that Area 1 contains:

$$\boldsymbol{z}_1 = \begin{bmatrix}\boldsymbol{z}_{1,2}^T & \boldsymbol{z}_{1,3}^T\end{bmatrix}^T.$$

At Step $(t+1)$, the ADMM procedure for one area is given as an example. Given the information from Aggregator 1 ($\boldsymbol{z}_{1,2}^t$) and Aggregator 2 ($\boldsymbol{z}_{1,3}^t$) as well as the dual variable vector $\boldsymbol{\lambda}_1^t$, the objective function for Area 1 is as follows.

$$\begin{aligned}L_1(\boldsymbol{x_1}; \boldsymbol{z_1^t}, \boldsymbol{\lambda_1^t}) = &\sum_{i \in \mathcal{G}_{A_1}} (f_P(P_{gi}) + f_Q(Q_{gi})) \\ +(\boldsymbol{\lambda}_1^t)^T(\boldsymbol{A}_1\boldsymbol{x}_1 - \boldsymbol{z}_1^t) &+ \frac{\rho}{2}\|\boldsymbol{A}_{1,2}\boldsymbol{x}_1 - \boldsymbol{z}_{1,2}^t\|^2 \\ &+\frac{\rho}{2}\|\boldsymbol{A}_{1,3}\boldsymbol{x}_1 - \boldsymbol{z}_{1,3}^t\|^2\end{aligned} \tag{2}$$

where $\boldsymbol{A}_{1,2}$ and $\boldsymbol{A}_{1,3}$ are permutation matrices that define the relationship between $\boldsymbol{z}_{1,2}$, $\boldsymbol{z}_{1,3}$ versus $\boldsymbol{x}_1$, respectively ($\boldsymbol{A}_{1,2} \in \mathbb{R}^{6\times 22}$ $\boldsymbol{A}_{1,3} \in \mathbb{R}^{4\times 22}$) and $\boldsymbol{A}_1 = \begin{bmatrix}\boldsymbol{A}_{1,2} \\ \boldsymbol{A}_{1,3}\end{bmatrix}$, and ρ is a positive constant and is termed as penalty factor for ADMM.

Inequality and equality constraints are given as follows.

$$\begin{aligned}&P_{gi}^{\min} \le P_{gi} \le P_{gi}^{\max}, \quad i \in \mathcal{G}_{A_1} \\ &Q_{gi}^{\min} \le Q_{gi} \le Q_{gi}^{\max}, \quad i \in \mathcal{G}_{A_1} \\ &V_i^{\min} \le |V_i| \le V_i^{\max}, \quad i \in \mathcal{N}_{A_1} \\ &P_i^g - P_i^d = \sum_j V_i V_j (G_{ij}\cos\theta_{ij} + B_{ij}\sin\theta_{ij}), i \in \mathcal{N}_{A_1} \\ &Q_i^g - Q_i^d = \sum_j V_i V_j (G_{ij}\sin\theta_{ij} - B_{ij}\cos\theta_{ij}), i \in \mathcal{N}_{A_1}\end{aligned} \tag{3}$$

where G_{ij} and B_{ij} are the real and imaginary components of the admittance matrix $\boldsymbol{Y}$'s element Y_{ij} and $\theta_{ij} = \theta_i - \theta_j$. .

Area 1 will solve the above optimization problem and find $\boldsymbol{x}_1^{t+1}$. Similarly, other areas also find their

solutions: $\boldsymbol{x}_2^{t+1}$ and $\boldsymbol{x}_3^{t+1}$. The update procedures in the three aggregators are as follows.

$$\begin{aligned}
\boldsymbol{z}_{1,2}^{t+1} &= \frac{1}{2}\left(\boldsymbol{A}_{1,2}\boldsymbol{x}_1^{t+1} + \boldsymbol{A}_{2,1}\boldsymbol{x}_2^{t+1}\right) \\
\boldsymbol{z}_{1,3}^{t+1} &= \frac{1}{2}\left(\boldsymbol{A}_{1,3}\boldsymbol{x}_1^{t+1} + \boldsymbol{A}_{3,1}\boldsymbol{x}_3^{t+1}\right) \\
\boldsymbol{z}_{1,3}^{t+1} &= \frac{1}{2}\left(\boldsymbol{A}_{2,3}\boldsymbol{x}_2^{t+1} + \boldsymbol{A}_{3,2}\boldsymbol{x}_3^{t+1}\right)
\end{aligned} \tag{4}$$

Each area now receives the aggregated information from the aggregators. The dual variables for each area will then be updated.

$$\begin{aligned}
\boldsymbol{\lambda}_1^{t+1} &= \boldsymbol{\lambda}_1^t + \rho(\boldsymbol{A}_1\boldsymbol{x}_1^{t+1} - \boldsymbol{z}_1^{t+1}) \\
\boldsymbol{\lambda}_2^{t+1} &= \boldsymbol{\lambda}_2^t + \rho(\boldsymbol{A}_2\boldsymbol{x}_2^{t+1} - \boldsymbol{z}_2^{t+1}) \\
\boldsymbol{\lambda}_3^{t+1} &= \boldsymbol{\lambda}_3^t + \rho(\boldsymbol{A}_3\boldsymbol{x}_3^{t+1} - \boldsymbol{z}_3^{t+1})
\end{aligned} \tag{5}$$

For this example, the auxiliary variable is at Area 1 is $\boldsymbol{A}_1\boldsymbol{x}_1$ while the consensus vectors are $\boldsymbol{z}_{1,2}$ and $\boldsymbol{z}_{1,3}$.

2.3. ADMM's General Formulation for AC OPF

With the small-scale example examined, we now proceed to define the procedure of consensus ADMM for a general AC OPF problem with K subareas and m aggregators. The set of the subareas is notated as $A = \{A_1, A_2, ..., A_K\}$. An aggregator collects information from two subareas and computes their average.

For Area k, the subproblem's decision variable vector is defined as $\boldsymbol{x}_k$ ($\boldsymbol{x}_k \subset \boldsymbol{x}$). The subproblem requires information from all aggregators that collect information from Area k. The consensus variable vector between A_i and A_j is defined as $\boldsymbol{z}_{i,j}$. Hence the auxiliary variable vector of Area k should include all information related to the consensus vectors. Let the set of the adjacent areas of Area k be defined as adj_k. Then $\boldsymbol{z}_{k,j}$ ($j \in adj_k$) is a consensus vector between Area k and its adjacent area j. Take the Area 1 in Figure 1 for example. Area 1 will not share the upper and lower bounds or the actual generation power of generations 1-3 to other agencies. What Area 2 and Area 3 can know is the bus voltage phasors on bus 4 and 5.

$$\boldsymbol{z}_k = \bigcup \boldsymbol{z}_{k,j}, \quad j \in adj_k.$$

At Step $(t+1)$, the subproblem solved at Area k is to minimize the augmented Lagrangian function of (6) with the consensus vector $\boldsymbol{z}_k^t$ and dual variable vector $\boldsymbol{\lambda}_k^t$ given from the previous step.

$$\min_{\boldsymbol{x}_k \in \mathcal{X}_k} \quad L_k(\boldsymbol{x_k}; \boldsymbol{z_k^t}, \boldsymbol{\lambda_k^t}) \tag{6}$$

where $\mathcal{X}_k$ is the feasible region defined by all the constraints related to Area k, and

$$\begin{aligned}
L_k(\boldsymbol{x_k}; \boldsymbol{z_k^t}, \boldsymbol{\lambda_k^t}) &= \sum_{i \in \mathcal{G}_{A_k}} (f_P(P_{gi}) + f_Q(Q_{gi})) \\
+(\boldsymbol{\lambda}_k^t)^T(\boldsymbol{A}_k\boldsymbol{x}_k - \boldsymbol{z}_k^t) &+ \sum_{j \in adj_k} \frac{\rho}{2}\|\boldsymbol{A}_{k,j}\boldsymbol{x}_k - \boldsymbol{z}_{k,j}^t\|^2.
\end{aligned} \tag{7}$$

At the aggregation step, each aggregator conducts averaging based on the information collected from the related two areas. The computing procedure at Step $(t+1)$ is summarized as follows.

$$\boldsymbol{x}_k^{t+1} = \underset{\boldsymbol{x}_k \in \mathcal{X}_k}{\operatorname{argmin}} L_k(\boldsymbol{x}_k; \boldsymbol{z}_k^t, \boldsymbol{\lambda}_k^t), \quad k = 1, \cdots, K \tag{8a}$$

$$\boldsymbol{z}_{i,j}^{t+1} = \frac{1}{2}(\boldsymbol{A}_{i,j}\boldsymbol{x}_i^{t+1} + \boldsymbol{A}_{j,i}\boldsymbol{x}_j^{t+1}), (i,j) \text{ for all aggregators} \tag{8b}$$

$$\boldsymbol{\lambda}_k^{t+1} = \boldsymbol{\lambda}_k^t + \rho(\boldsymbol{A}_k\boldsymbol{x}_k^{t+1} - \boldsymbol{z}_k^{t+1}), \quad k = 1, \cdots, K \tag{8c}$$

Both $\boldsymbol{x}$ and $\boldsymbol{z}$ are solved through optimization procedure. Due to the particular structure of consensus ADMM, the consensus variable z's solution at each step can be found by using averaging [8].

In this paper, we directly implement consensus ADMM's algorithm into OPF. Equations (4) and (8b) are the averaging step for consensus variable update. The implementation strictly follows consensus ADMM and hence it is guaranteed to lead to optimality should the original problem is a convex problem. Since the problem we are dealing with is a nonconvex problem, achieving convergence is tricky. That is the reason that several techniques are adopted in the paper, including introduction of auxiliary variables, network partitioning strategy and penalty factor updating.

3. New Auxiliary Variables for Convergence Improvement

A major challenge of the ADMM formulation presented in Section II is its slow convergence speed. This issue has been identified in the literature [22]. [22] presents two techniques to improve the convergence speed. One is to vary the penalty factor ρ. The other is to use auxiliary variable. The latter can lead to more significant improvement in convergence.

In this section, the auxiliary variable technique in [22] will be first described. We then present our new auxiliary variable technique. With the introduction of the new auxiliary variables, the ADMM procedure is revisited. In addition, penalty factor updating technique is also incorporated.

3.1. Auxiliary variables in [22]

We again use the two areas in Fig. 2 for explanation. In order to make sure the duplicated voltages converging to a same value, the constraints $\overline{V}_{i,1} = \overline{V}_{i,2}$, $\overline{V}_{j,1} = \overline{V}_{j,2}$ should be enforced through the consensus ADMM process. In [22, 23], the equivalent constraints are given as

$$\overline{V}_{i,1} - \overline{V}_{j,1} = \overline{V}_{i,2} - \overline{V}_{j,2}, \quad \overline{V}_{i,1} + \overline{V}_{j,1} = \overline{V}_{i,2} + \overline{V}_{j,2}. \tag{9}$$

The auxiliary variables in Area 1 are defined as

$$\boldsymbol{z}_1 = \begin{bmatrix} \boldsymbol{z}^-_{ij,1} \\ \boldsymbol{z}^+_{ij,1} \end{bmatrix} = \boldsymbol{A}_1 \boldsymbol{x}_1 \tag{10}$$

where

$$\boldsymbol{z}^-_{ij,1} = \beta^-(\overline{V}_{i,1} - \overline{V}_{j,1}), \quad \boldsymbol{z}^+_{ij,1} = \beta^+(\overline{V}_{i,1} + \overline{V}_{j,1}) \tag{11}$$

β^- and β^+ are set to be $\beta^- \gg \beta^+ > 0$, which gives more weight to $\overline{V}_{i,1} - \overline{V}_{j,1}$ since it is strongly related to the power flow through tie-line $i-j$. The consensus condition between area 1 and 2 is given in (12).

$$\boldsymbol{z}^-_{ij,1} = -\boldsymbol{z}^-_{ji,2}, \quad \boldsymbol{z}^+_{ij,1} = \boldsymbol{z}^+_{ji,2} \tag{12}$$

3.2. Proposed auxiliary variables

Inspired by the above idea on auxiliary variable definition, we reexamine the power flow expression on the tie-line $i-j$ and aim to designate a new set of auxiliary variables for further convergence improvement. Notate the branch index of this line as k. Assume that the line is represented by a π circuit with the series admittance $y_k = 1/(R_k + jX_k)$ and two shunt admittances $jb_k/2$. The complex power flowing from Bus i to Bus j is:

$$S_{ij} = \left(y_k^* + j\frac{b_k}{2}\right) V_i^2 + y_k^* \overline{V}_i \overline{V}_j^*. \tag{13}$$

Instead of enforcing $\overline{V}_{i,1} = \overline{V}_{i,2}$, $\overline{V}_{j,1} = \overline{V}_{j,2}$, we opt to enforce

$$\overline{V}_{i,1}\overline{V}^*_{j,1} = \overline{V}_{i,2}\overline{V}^*_{j,2}.$$

Note the original constraints have two equality constraints of complex variables or four equality constraints in the real domain. The new constraint, however, has only one equality constraint in the complex domain or two constraints in the real domain. We add two more constraints:

$$V_{i,1}^2 = V_{i,2}^2, \quad V_{j,1}^2 = V_{j,2}^2.$$

The new set can then replace the old set. Note the newly introduced auxiliary variables are indeed the decision variables of second-order conic relaxation (SOCP) relaxation of AC OPF [9].

Instead of using the polar form of voltage phasor, we now use the rectangular form of voltage phasor ($\overline{V}_i = e_i + jf_i$) to avoid trigonometric functions such as $\cos\theta_{ij}$. The new set of variables related to a tie-line are defined as follows.

$$\begin{aligned} c_{ii} &= V_i^2 = e_i^2 + f_i^2 \\ c_{jj} &= V_j^2 = e_j^2 + f_j^2 \\ c_{ij} &= V_i V_j \cos(\theta_i - \theta_j) = e_i e_j + f_i f_j \\ s_{ij} &= V_i V_j \sin(\theta_i - \theta_j) = f_i e_j - e_i f_j \end{aligned} \tag{14}$$

To achieve consensus between Area 1 and Area 2, the following constraints should be met.

$$c_{ii,1} = c_{ii,2},\ c_{jj,1} = c_{jj,2},\ c_{ij,1} = c_{ji,2},\ s_{ij,1} = -s_{ji,2} \tag{15}$$

One more step is carried out to make sure that each auxiliary variable contains the information from Bus i and Bus j. Hence, the first two variables will be replaced by their sum and difference. Finally, the two auxiliary variable vectors m_{12}^+ and m_{12}^- are found and presented in (16).

$$m_{12}^- = \beta^- \begin{bmatrix} c_{ii,1} - c_{jj,1} \\ s_{ij,1} \end{bmatrix} \tag{16a}$$

$$m_{12}^+ = \beta^+ \begin{bmatrix} c_{ii,1} + c_{jj,1} \\ c_{ij,1} \end{bmatrix} \tag{16b}$$

where β^- and β^+ are multiplier factors to give more weight on z^-, which providing convergence on an approximate linear problem on power flow on tie-lines. Therefore, the consensus vector between Area 1 and Area 2 can be expressed as

$$\boldsymbol{m}_{1,2} = \begin{bmatrix} m_{12}^- \\ m_{12}^+ \end{bmatrix} \tag{17}$$

Note that with our proposed auxiliary variables, we no longer have the linear relationship between the primary decision variables $\boldsymbol{x}_k$ and the exchanging information $\boldsymbol{z}_k$. A corresponding $\boldsymbol{m}_k$ will be created based on $\boldsymbol{x}_k$ to aggregate all exchanging information from Area k. The consensus constraint is $\boldsymbol{m}_k = \boldsymbol{z}_k$ for area k, where $\boldsymbol{z}_k$ is defined as the consensus variable vector for Area k.

3.3. ADMM Based on Proposed Auxiliary Variables

The brief algorithm of the proposed ADMM AC OPF is summarized in Algorithm 1. For initialization in line 2, we use 1 pu voltage magnitude, random phase angles to set all voltage phasors in rectangular form. We properly choose ρ_{k0} to compromise of better convergence and less gap. Note that the exchange message $\boldsymbol{m}$ in line 6 is prepared for all the neighbors of local area k. The weighting factors β^- and β^+ should be chosen in a way that $\beta^- \gg \beta^+ > 0$.

To enhance the ADMM convergence performance, penalty parameter $\boldsymbol{\rho}$ updating principle, detailed in [22], is added after λ update. We increase the penalty parameter only if the primal gap is not decreasing sufficiently. We first check the primal gap decrease in area k via

$$\boldsymbol{\rho}_k^{t+1} = \begin{cases} \boldsymbol{\rho}_k^{t+1} & \text{if } \Gamma_k^{t+1} \le \gamma \Gamma_k^t \\ \tau \boldsymbol{\rho}_k^t & \text{otherwise} \end{cases} \tag{18}$$

Algorithm 1: New auxiliary variable ADMM AC OPF

Input : Partitioning the power system into K areas

Initialize: Local variables $\boldsymbol{x}_{k0}$, auxiliary variable $\boldsymbol{z}_{k0}$, Lagrange multipliers $\boldsymbol{\lambda}_{k0}$ and penalty parameters $\boldsymbol{\rho}_{k0}$

while *Step*$= t$ & *Gap*$_{max} \geq$ *threshold* **do**

  for *area* $k = 1$ *to* K **do**

    Update local variables $\boldsymbol{x}_{k+1}^{t}$ via:

$$\boldsymbol{x}_{k}^{t+1} = \underset{\boldsymbol{x}_k \in \mathcal{X}_k}{\operatorname{argmin}} \quad L_k(\boldsymbol{x}_k; \boldsymbol{z}_k^t, \boldsymbol{\lambda}_k^t, \boldsymbol{\rho}_k^t)$$

    Prepare exchange messages between every adjacent area: $h \in adj_k$ based on solved $\boldsymbol{x}_k^{t+1}$. If there is only one tie-line $i-j$ between the two areas, then:

$$\boldsymbol{m}_{k,h}^{t+1} = \begin{bmatrix} \beta^{-} \begin{bmatrix} c_{ii,k}^{t+1} - c_{jj,k}^{t+1} \\ s_{ij,k}^{t+1} \end{bmatrix} \\ \beta^{+} \begin{bmatrix} c_{ii,k}^{t+1} + c_{jj,k}^{t+1} \\ c_{ij,k}^{t+1} \end{bmatrix} \end{bmatrix}$$

  end

  for *all adjacent areas* **do**

    Update consensus variables $\boldsymbol{z}_{k,h}$:

$$(\boldsymbol{z}_{k,h}^{-})^{(t+1)} = \frac{1}{2}\left((\boldsymbol{m}_{k,h}^{-})^{(t+1)} - (\boldsymbol{m}_{h,k}^{-})^{(t+1)}\right)$$

$$(\boldsymbol{z}_{k,h}^{+})^{(t+1)} = \frac{1}{2}\left((\boldsymbol{m}_{k,h}^{+})^{(t+1)} + (\boldsymbol{m}_{h,k}^{+})^{(t+1)}\right)$$

  end

  for *area k=1 to K, Update Lagrange multipliers via:* **do**

$$\boldsymbol{\lambda}_{k}^{t+1} = \boldsymbol{\lambda}_{k}^{t} + \boldsymbol{\rho}_{k}^{t}(\boldsymbol{m}_{k}^{t+1} - \boldsymbol{z}_{k}^{t+1})$$

    Update the local gap via:

$$\Gamma_{k}^{t+1} = ||\boldsymbol{m}_{k}^{t+1} - \boldsymbol{z}_{k}^{t+1}||_{\infty}$$

    Update local penalty parameters via:

$$\boldsymbol{\rho}_{k}^{t+1} = \begin{cases} \boldsymbol{\rho}_{k}^{t+1} & \text{if } \Gamma_{k}^{t+1} \leq \gamma \Gamma_{k}^{t} \\ \tau \boldsymbol{\rho}_{k}^{t} & \text{otherwise} \end{cases}$$

    Correct local penalty parameters via:

$$\boldsymbol{\rho}_{k}^{t+1} = \max(\boldsymbol{\rho}_{k}^{t+1}, \quad \boldsymbol{\rho}_{h}^{t+1})$$

  end

end

with constants $0 < \gamma < 1$ and $\tau > 1$, and with a measure of the primal gap (in infinity norm) in (19):

$$\Gamma_{k}^{t+1} = ||\boldsymbol{m}_{k}^{t+1} - \boldsymbol{z}_{k}^{t+1}||_{\infty} \tag{19}$$

The penalty parameter updating constants γ and τ should be set close to 1 to avoid a rapid increase in

penalty parameters. Tuning ADMM parameters is depended on empirical studies. Reference [28] gives some selection rules on turning ADMM parameters for specific problems.

Eq. (20) is to select the larger ρ between any two neighbor areas, e.g. k and h.

$$\boldsymbol{\rho}_k^{t+1} = \max(\boldsymbol{\rho}_k^{t+1}, \quad \boldsymbol{\rho}_h^{t+1}) \tag{20}$$

4. Spectral Partitioning

To automatically partition a power network with N buses, we use spectral clustering technique. Our objective is to have multiple subareas. The buses inside the same subarea are tightly connected while any two subareas are connected less tightly. The admittance matrix $\boldsymbol{Y}$ of a power grid can represent the bus connectivity. If two buses (i and j) are tightly connected, then a large magnitude of Y_{ij} is expected. If they are loosely connected, a small magnitude of Y_{ij} is expected. If they are not connected, then the admittance is zero ($Y_{ij} = 0$).

To apply the spectral clustering technique, a graph Laplacian L is required and its eigenvalues and eigenvalues will be computed. If a grid will be divided into K subareas, then the first K eigenvectors corresponding to the first K eigenvalues ($0 = \lambda_1 \leq \lambda_2 \leq \cdots \lambda_K \leq \cdots \leq \lambda_N$) will be used for clustering. A tutorial on spectral clustering can be find in [29].

We first obtain an adjacent matrix $\boldsymbol{W}$ with its diagonal elements as 0 and non-diagonal elements as the absolute values from the $\boldsymbol{Y}$ matrix:

$$\boldsymbol{W} = \begin{bmatrix} 0 & |Y_{1,2}| & \dots & |Y_{1,N}| \\ |Y_{2,1}| & 0 & \dots & |Y_{2,N}| \\ \vdots & \vdots & \ddots & \vdots \\ |Y_{N,1}| & |Y_{N,2}| & \dots & 0 \end{bmatrix} \tag{21}$$

The Graph Laplacians (L) will be built as follows.

$$\boldsymbol{L} = \boldsymbol{D} - \boldsymbol{W} \tag{22}$$

where $\boldsymbol{D}$ is a diagonal matrix and its i^{th} diagonal component is notated as d_i where $d_i = \sum_j W_{ij}$.

The Laplacian matrix will be normalized:

$$\boldsymbol{L}_{\text{sym}} = \boldsymbol{D}^{-1/2}\boldsymbol{L}\boldsymbol{D}^{-1/2} \tag{23}$$

The i^{th} eigenvalue λ_i and eigenvectors v_i have the following relationship (24):

$$\boldsymbol{L}_{\text{sym}} v_i = \lambda_i v_i. \tag{24}$$

Since $\boldsymbol{L}_{\text{sym}}$ is symmetric, the eigenvalues are real and non-negative. These eigenvalues are also called as the spectrum of the normalized Laplacian.

The first K eigenvectors will be used to form a $N \times K$ matrix $\boldsymbol{V}$:

$$\boldsymbol{V} = \begin{bmatrix} v_1 & v_2 & \cdots & v_K \end{bmatrix}. \tag{25}$$

We then apply the k-means clustering algorithm on $\boldsymbol{V}$. $\boldsymbol{V}$'s each row is a data point and there are N data points. The k-means clustering algorithm tries to group the$N$ data points to K groups. The clustering is conducted in a heuristic approach described as follows.

1. Randomly choose K cluster centroids $c_j, j = 1, \cdots, K$.
2. Assign each data point to one of the clusters with closest Euclidean distance. The objective is to

minimize the sum of the Euclidean distances from a data point to its cluster's centroid.

$$J = \min \sum_{j=1}^{K} \sum_{i \in S_j} ||y_i - c_j||^2 \tag{26}$$

where S_j is the set of data points that are assigned to j^{th} cluster, y_i is the i^{th} row of $\boldsymbol{V}$.

3. Based on the assignment of data points to each cluster, recalculate the centroids for each cluster.
4. Repeat step 2 and 3 until the the new centroids do not differ from the old ones.

The MATLAB spectral partitioning toolbox [30] is used in this research. The toolbox gives partitioning results based on both the graph Laplacian or its normalized matrix. The normalization step can improve the convergence in the k-means process. For example, it can reduce the iterations from 9 to 4 in partitioning IEEE 300-bus network. Two example network partitioning results are listed in Table 1.

5. Case Study Results

In this section, we present case study results and a comparison between our proposed auxiliary variables-based approach and the existing approach in the literature. First, spectral partitioning of system network is conducted. Second, each AC OPF is solved using the proposed ADMM procedure. Parameter setting is presented. The convergence performance and AC OPF solutions of new proposed auxiliary variables-based ADMM are compared with those based on ADMM in the literature. The performance will be discussed through comparing with the auxiliary variables setting in [23]. Additionally, the effect of partitioning number will be presented.

5.1. Parameter Settings

All the local variables $\boldsymbol{x}_{k0}$ are set to random values within the upper and lower bounds. We make sure the initial voltage magnitudes are 1 pu. The consensus variables $\boldsymbol{z}_{k0}$ are set to have 1 pu voltage magnitudes. The initial Lagrange multipliers $\boldsymbol{\lambda}_{k0}$ are set to zeros.

The proposed new auxiliary variable-based ADMM will be compared with the ADMM in [22, 23]. Same parameter settings are used. The penalty parameters ρ_{k0} are set to be large enough to guarantee the convergence. Its incremental step size τ and γ are set as $\tau > 1$ and $0 < \gamma < 1$, respectively. As a rule of thumb, it is highly possible to find a better solution if both τ and γ are set closer to 1, but it will take more iterations to reach the threshold generally. In our cases, most cases are tested in $\tau = 1.05$ and $\gamma = 0.9$, except the 1354-bus network. The weighting constants should be chosen in such a way that $\beta^- \gg \beta^+ > 0$. Here, $\beta^- = 1$, $\beta^+ = \dfrac{1}{5}$. The threshold of error for convergence check is selected at 10^{-5}, which is the maximum mismatch of $\|\boldsymbol{m}_k - \boldsymbol{z}_k\|_\infty$ among all areas.

To individualize the impact of penalty factor and proposed auxiliary variable, we carried out three case studies on 14-bus system. In first two scenarios, we show that increasing penalty factor ρ by five times makes convergence faster and the iteration steps reduce from 35 to 23 to achieve a tolerance of 10^{-3}. In the third scenario, we show that by introducing the proposed auxiliary variables, with the penalty factor intact, the iteration steps reduce from 35 to 13. The plots are presented in Fig. 4. This set of studies indicate that larger penalty factor results in a faster convergence while using auxiliary variables results in even faster convergence. The effect of auxiliary variable on convergence is more significant compared to that of the penalty factor.

5.2. Convergence Performance

In Table 2, all relevant parameter settings and final solutions are listed. The results that area generated by the centralized AC OPF using MATPOWER [31] are given first. Two ADMM methods are compared: our proposed auxiliary variable-based ADMM and the existing auxiliary variable-based ADMM in [22, 23]. Note that we applied the spectral clustering algorithm to generate the same partition result for each case.

The objective functions, constraints, parameter settings, and penalty factor updating algorithm are the same for the two methods. The only difference is the definition of the auxiliary variables. Both ADMM methods generate comparable objective values. Their differences to the MATPOWER results notated as gap are comparable. It can be seen that the computational cost per iteration of the proposed ADMM increases slightly from the method in [22, 23] while the iteration steps reduce. This is due to a more demanding use of auxiliary variables. The overall computational cost for two approaches are comparable.

In Fig. 5, the voltage phasor on each bus ($\overline{V}$), power generation(P_g, Q_g), objective function value and maximal mismatch ($||\boldsymbol{m}_k - \boldsymbol{z}_k||_\infty$) of the proposed ADMM are presented for IEEE 30-, 57-, 118-, 300- and 1354-bus power systems, respectively.

The first column presents the voltage outputs from both our proposed ADMM and MATPOWER. The second column presents P_g and Q_g. It can be seen that those variables converge.

The 3$^{\text{rd}}$ and 4$^{\text{th}}$ columns present objective values and maximal mismatch. A comparison of the effect of our proposed auxiliary variables versus that of the existing auxiliary variable [23] is made in these two columns. Note in [23], the auxiliary and consensus variables are defined differently from our paper. The mismatches compared are referring to the same set of variables. It can be clearly seen that the proposed ADMM shows significant improvement on ADMM convergence in most cases. Especially on 57-bus, 300-bus, and 1354-bus networks, the mismatch of proposed method converged faster than another one.

5.3. Impact of Partition Numbers

To test the flexibility and robustness of our spectral partitioning with new auxiliary ADMM method, we used various partitioning scenarios for the IEEE 300-bus system. In the following tests, the 300-bus network is partitioned into 10, 20, 30, 40 and 50 areas, respectively. All the parameter settings are identical.

Fig. 6 presents two figures to demonstrate the performance of proposed auxiliary variables-based ADMM for different numbers of partitioning areas. Based on the plots of the objective values, we can see that the final optimal results are very close to each other for different partitioning scenarios. The mismatch plots show that similar iteration numbers are required to achieve 10^{-5} threshold under different partitions. Hence, our algorithm is robust against partitioning areas.

6. Conclusion

In this paper, we proposed new auxiliary variables for information exchange in ADMM for large-scale nonconvex AC OPF solving. The new auxiliary variables are proposed based on the tie-line power flow expressions. They align with the decision variables used in SOCP relaxation of AC OPF. Unlike the existing auxiliary variables, the new auxiliary variables are not linearly related to the local decision variables. We present a clear information structure of the proposed ADMM and compared the new auxiliary variables-based ADMM with the exiting auxiliary variables-based ADMM. Significant improvement has been demonstrated for all test cases.

[1] D. K. Molzahn, F. Dörfler, H. Sandberg, S. H. Low, S. Chakrabarti, R. Baldick, and J. Lavaei, "A survey of distributed optimization and control algorithms for electric power systems," *IEEE Transactions on Smart Grid*, vol. 8, no. 6, pp. 2941–2962, 2017.

[2] V. R. Disfani, L. Fan, L. Piyasinghe, and Z. Miao, "Multi-agent control of community and utility using lagrangian relaxation based dual decomposition," *Electric Power Systems Research*, vol. 110, pp. 45–54, 2014.

[3] B. H. Kim and R. Baldick, "Coarse-grained distributed optimal power flow," *IEEE Transactions on Power Systems*, vol. 12, no. 2, pp. 932–939, 1997.

[4] ——, "A comparison of distributed optimal power flow algorithms," *Power Systems, IEEE Transactions on*, vol. 15, no. 2, pp. 599–604, 2000.

[5] Z. Miao and L. Fan, "A novel multi-agent decision making architecture based on dual's dual problem formulation," *IEEE Transactions on Smart Grid*, 2016.

[6] E. Dall'Anese, H. Zhu, and G. B. Giannakis, "Distributed optimal power flow for smart microgrids," *IEEE Transactions on Smart Grid*, vol. 4, no. 3, pp. 1464–1475, 2013.

[7] T. Erseghe, "Distributed optimal power flow using ADMM," *IEEE transactions on power systems*, vol. 29, no. 5, pp. 2370–2380, 2014.

[8] S. Boyd, N. Parikh, E. Chu, B. Peleato, and J. Eckstein, "Distributed optimization and statistical learning via the alternating direction method of multipliers," *Foundations and Trends® in Machine Learning*, vol. 3, no. 1, pp. 1–122, 2011.

[9] R. A. Jabr, "Radial distribution load flow using conic programming," *IEEE transactions on power systems*, vol. 21, no. 3, pp. 1458–1459, 2006.
[10] Q. Peng and S. H. Low, "Distributed algorithm for optimal power flow on a radial network," in *Decision and Control (CDC), 2014 IEEE 53rd Annual Conference on*. IEEE, 2014, pp. 167–172.
[11] ——, "Distributed algorithm for optimal power flow on an unbalanced radial network," in *Decision and Control (CDC), 2015 IEEE 54th Annual Conference on*. IEEE, 2015, pp. 6915–6920.
[12] ——, "Distributed optimal power flow algorithm for radial networks, i: Balanced single phase case," *IEEE Transactions on Smart Grid*, 2016.
[13] M. Ma, L. Fan, and Z. Miao, "Consensus ADMM and proximal ADMM for economic dispatch and AC OPF with SOCP relaxation," in *North American Power Symposium (NAPS), 2016*. IEEE, 2016, pp. 1–6.
[14] R. Madani, S. Sojoudi, and J. Lavaei, "Convex relaxation for optimal power flow problem: Mesh networks," *IEEE Transactions on Power Systems*, vol. 30, no. 1, pp. 199–211, 2015.
[15] E. DallAnese, S. V. Dhople, B. B. Johnson, and G. B. Giannakis, "Decentralized optimal dispatch of photovoltaic inverters in residential distribution systems," *IEEE Transactions on Energy Conversion*, vol. 29, no. 4, pp. 957–967, 2014.
[16] T. Erseghe and S. Tomasin, "Power flow optimization for smart microgrids by SDP relaxation on linear networks," *IEEE Transactions on Smart Grid*, vol. 4, no. 2, pp. 751–762, 2013.
[17] J. Lavaei and S. H. Low, "Zero duality gap in optimal power flow problem," *IEEE Transactions on Power Systems*, vol. 27, no. 1, pp. 92–107, 2012.
[18] S. Magnússon, P. C. Weeraddana, and C. Fischione, "A distributed approach for the optimal power-flow problem based on ADMM and sequential convex approximations," *IEEE Transactions on Control of Network Systems*, vol. 2, no. 3, pp. 238–253, 2015.
[19] R. Madani, A. Kalbat, and J. Lavaei, "ADMM for sparse semidefinite programming with applications to optimal power flow problem," in *Decision and Control (CDC), 2015 IEEE 54th Annual Conference on*. IEEE, 2015, pp. 5932–5939.
[20] B. A. Robbins, H. Zhu, and A. D. Domínguez-García, "Optimal tap setting of voltage regulation transformers in unbalanced distribution systems," *IEEE Transactions on Power Systems*, vol. 31, no. 1, pp. 256–267, 2016.
[21] R. Kar, Z. Miao, M. Zhang, and L. Fan, "ADMM for nonconvex ac optimal power flow," in *North American Power Symposium (NAPS)*. IEEE, 2017.
[22] T. Erseghe, "A distributed approach to the opf problem," *EURASIP Journal on Advances in Signal Processing*, vol. 2015, no. 1, p. 45, 2015.
[23] J. Guo, G. Hug, and O. K. Tonguz, "A case for non-convex distributed optimization in large-scale power systems," *IEEE Transactions on Power Systems*, 2016.
[24] G. A. Ezhilarasi and K. Swarup, "Network partitioning using harmony search and equivalencing for distributed computing," *Journal of Parallel and Distributed Computing*, vol. 72, no. 8, pp. 936–943, 2012.
[25] E. Cotilla-Sanchez, P. D. Hines, C. Barrows, S. Blumsack, and M. Patel, "Multi-attribute partitioning of power networks based on electrical distance," *IEEE Transactions on Power Systems*, vol. 28, no. 4, pp. 4979–4987, 2013.
[26] R. J. Sánchez-García, M. Fennelly, S. Norris, N. Wright, G. Niblo, J. Brodzki, and J. W. Bialek, "Hierarchical spectral clustering of power grids," *IEEE Transactions on Power Systems*, vol. 29, no. 5, pp. 2229–2237, 2014.
[27] J. Guo, G. Hug, and O. K. Tonguz, "Intelligent partitioning in distributed optimization of electric power systems," *IEEE Transactions on Smart Grid*, vol. 7, no. 3, pp. 1249–1258, 2016.
[28] E. Ghadimi, A. Teixeira, I. Shames, and M. Johansson, "Optimal parameter selection for the alternating direction method of multipliers (ADMM): quadratic problems," *IEEE Transactions on Automatic Control*, vol. 60, no. 3, pp. 644–658, 2015.
[29] U. Von Luxburg, "A tutorial on spectral clustering," *Statistics and computing*, vol. 17, no. 4, pp. 395–416, 2007.
[30] I. Bürk, "Spectral clustering," *Bachelor thesis, Universität Stuttgart*, 2012.
[31] R. D. Zimmerman and C. E. Murillo-Sánchez, "Matpower 4.1 users manual," *Power Systems Engineering Research Center, Cornell University, Ithaca, NY*, 2011.

List of Tables

Table 1: Spectral partitioning results of two networks

IEEE 14-bus 3 areas	{1-5}; {7-10}; {6, 11-14}	IEEE 30-bus 5 areas	{1-8, 28}; {9-11, 17, 21-22}; {12-16,23}; {18-20}; {24-27, 29-30}

Table 2: Case study results

Case	MATPOWER Min Cost ($hr)	ADMM	Min Cost ($hr)	Gap	Areas	ρ_{k0}	β^-	β^+	γ	τ	Ave time per area (s)	Iterations
30-bus	574.52	[22]	577.31	0.48%	5	1×10^5	1	1/5	0.9	1.05	0.41	87
		Proposed	**577.87**	**0.58%**	**5**	1×10^5	**1**	1/5	**0.9**	**1.05**	**0.79**	**63**
57-bus	41758.18	[22]	41758.18	0.04%	7	3×10^5	1	1/5	0.9	1.05	0.94	151
		Proposed	**41752.90**	**0.03%**	**7**	3×10^5	**1**	1/5	**0.9**	**1.05**	**0.91**	**113**
118-bus	129660.70	[22]	130240.66	0.44%	20	5×10^5	1	1/5	0.9	1.05	1.03	155
		Proposed	**130144.07**	**0.37%**	**20**	5×10^5	**1**	1/5	**0.9**	**1.05**	**1.16**	**123**
300-bus	719725.11	[22]	720031.57	0.04%	30	5×10^5	1	1/5	0.9	1.05	0.80	182
		Proposed	**719833.33**	**0.01%**	**30**	5×10^5	**1**	1/5	**0.9**	**1.05**	**1.22**	**148**
1354-bus	74060.41	[22]	74453.89	0.53%	60	5×10^5	1	1/5	0.99	1.02	2.44	226
		Proposed	**74472.94**	**0.55%**	**60**	5×10^5	**1**	1/5	**0.99**	**1.02**	**3.53**	**180**

List of Figures

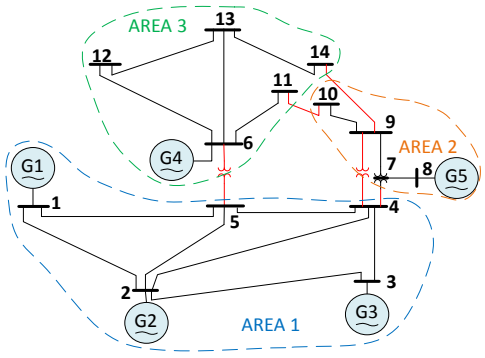

Figure 1: IEEE 14-bus is partitioned into 3 areas.

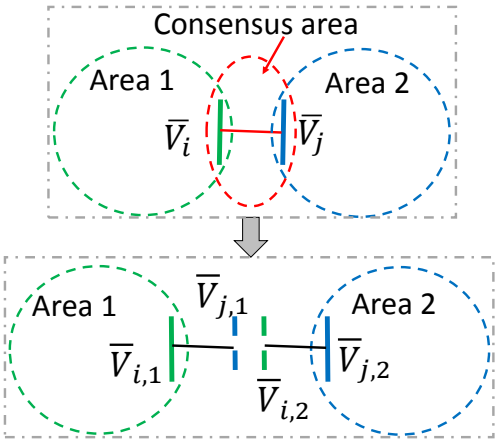

Figure 2: Subsystem decoupling.

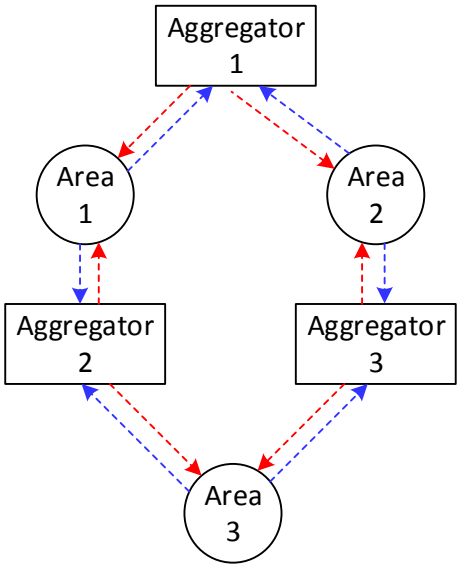

Figure 3: Information exchange structure.

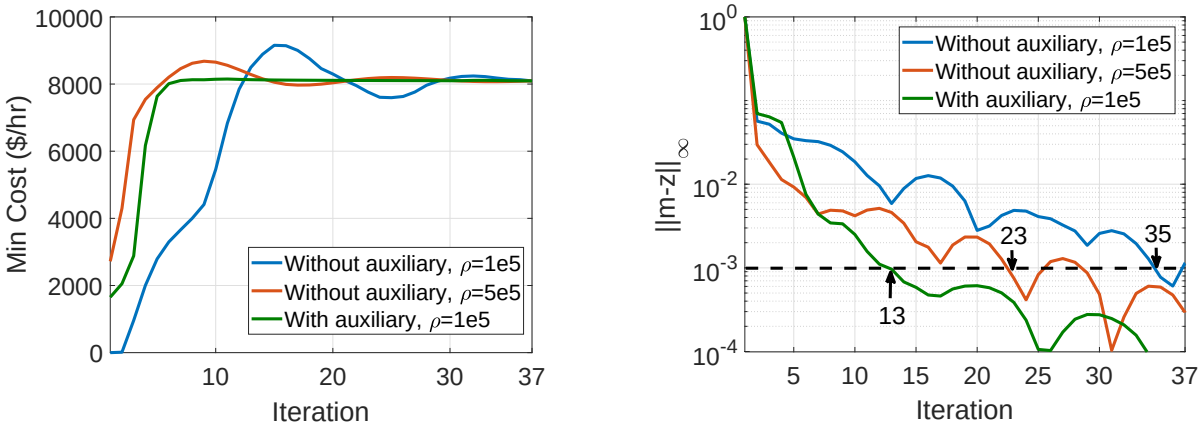

Figure 4: Convergence performances of 14-bus 3-area ADMM.

IEEE 30-bus network, 5 areas:

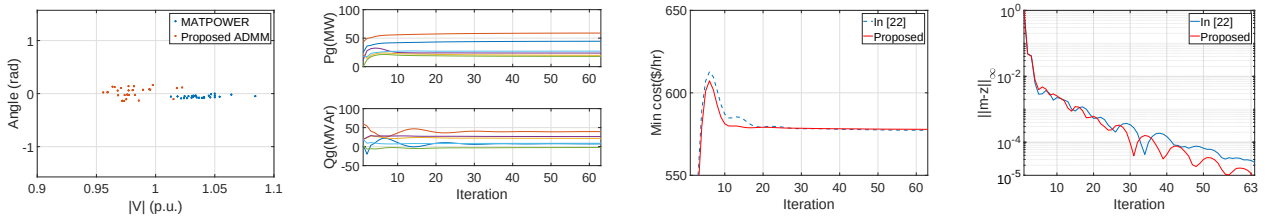

IEEE 57-bus network, 7 areas:

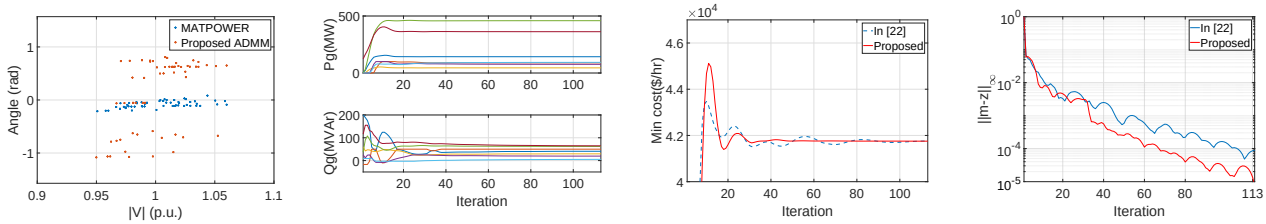

IEEE 118-bus network, 20 areas:

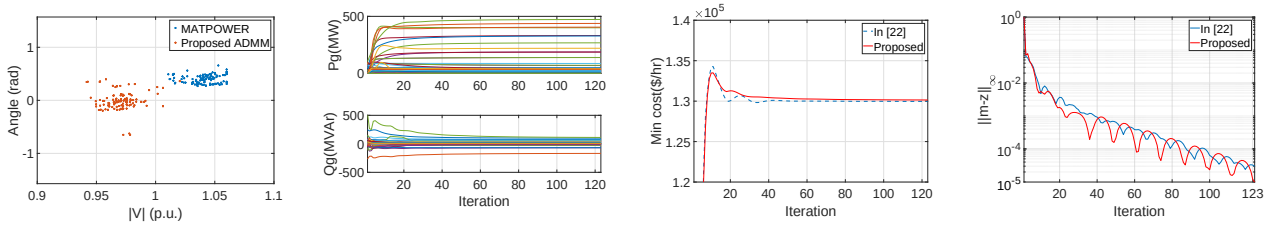

IEEE 300-bus network, 30 areas:

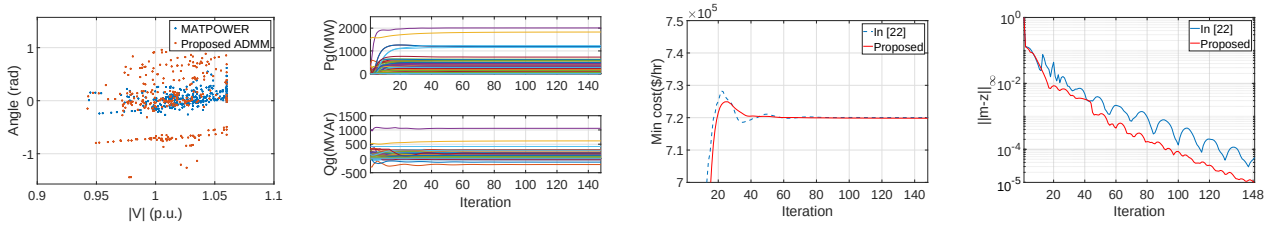

IEEE 1354-bus network, 60 areas:

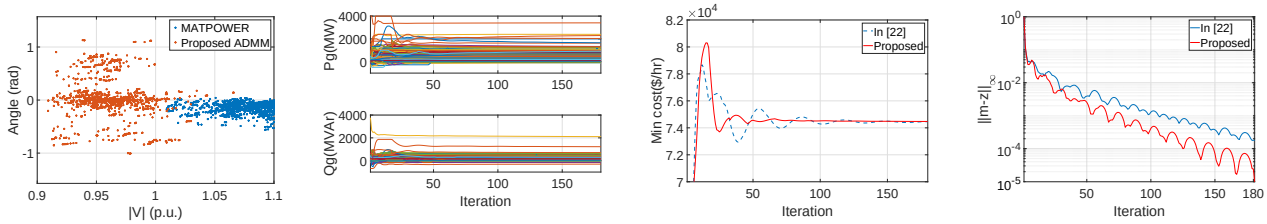

Figure 5: Performance of the new auxiliary variable-based ADMM.

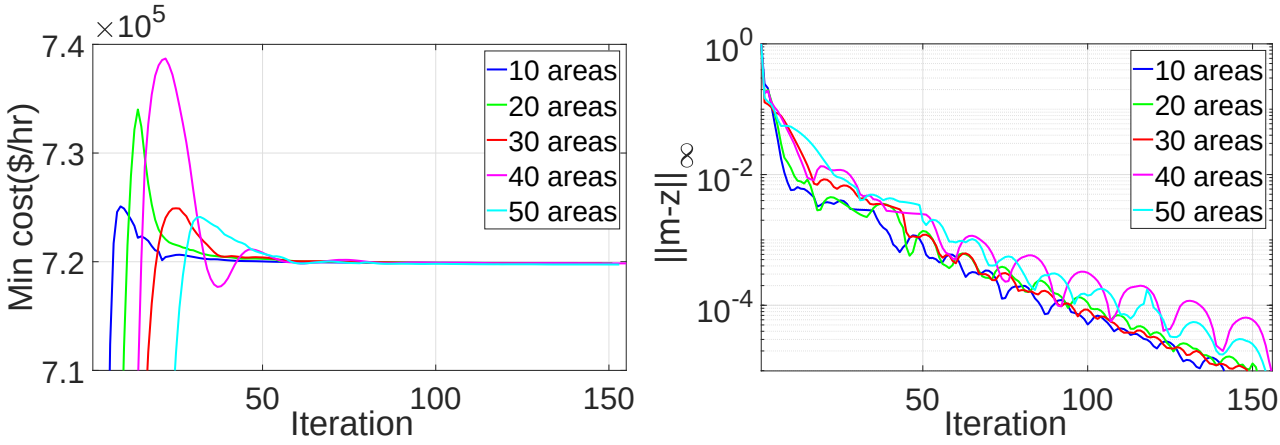

(a) Objective value

(b) Maximum mismatch

Figure 6: Proposed ADMM for different number of areas.